The route to stable lead-free double perovskites with the electronic structure of $MAPbI_3$: A case for mixed-cation $(Cs/MA/FA)_2InBiBr_6$ [MA = CH_3NH_3, FA = $CH(NH_2)_2$]

George Volonakis,[†] Amir Abbas Haghighirad,[‡] Henry J. Snaith,[‡] and Feliciano Giustino[*,†]

†*Department of Materials, University of Oxford, Parks Road OX1 3PH, Oxford, UK*

‡*Department of Physics, Clarendon Laboratory, University of Oxford, Parks Road, Oxford OX1 3PU, United Kingdom*

E-mail: feliciano.giustino@materials.ox.ac.uk

Phone: (+44) 01865 272380

Abstract

During the past two years $A_2BB'X_6$ halide double perovskites attracted attention as potential lead-free alternatives to Pb-based halide perovskites. However, none of the compounds discovered so far can match the optoelectronic properties of $MAPbI_3$ ($MA = CH_3NH_3$). Here we argue that, from the electronic structure viewpoint, the only option to make Pb-free double perovskites with electronic and optical properties similar to $MAPbI_3$ is to combine In and Bi as B^+ and B^{3+} cations, respectively. While inorganic double perovskites such as Cs_2InBiX_6 were found to be unstable due to the tendency of In^+ to oxidize into In^{3+}, here we show that it is possible to stabilize In-based halide double perovskites by increasing the size of the A-site cation. In fact, by performing first-principles calculations of phase stability and decomposition pathways, we found that the +1 oxidation state of In becomes progressively more stable as the A-site cation changes from K to Cs, and the structure is predicted to be stable for cations larger than Cs. Based on these results we propose the use of organic cations MA and FA [$FA = CH(NH_2)_2$] as the most promising route to stabilize $A_2InBiBr_6$ double perovskites. We show that the electronic and optical properties of $MA_2InBiBr_6$ are remarkably similar to those of the champion compound $MAPbI_3$, and we explore the effects of combining Cs, MA, and FA to form mixed-cation $(Cs/MA/FA)_2InBiBr_6$ halide double perovskites.

Perovskites find applications in many areas of technology due to their remarkable structural, electronic, optical, electrical, magnetic, catalytic, and superconducting properties.[1–7] During the past five years hybrid organic-inorganic ABX_3 perovskites using lead as the B-site cation and halogens (I, Br, Cl) as the X-site anions revolutionized the research on photovoltaics.[1,8–10] The solar-to-electricity power conversion efficiency of devices based on (MA/FA)PbI_3 and related systems, with MA = CH_3NH_3 and FA = $CH(NH_2)_2$, currently above 22%,[11] exceeds the performance of amorphous and multi-crystalline thin film silicon cells. However, lead halide perovskites tend to degrade when exposed to air, heat, or humidity,[12] therefore the fabrication of solar modules requires more complex encapsulation strategies than for silicon. In addition, the presence of lead in these materials raises questions on the environmental impact in view of the large-scale deployment of perovskite solar cells.

So far the quest for efficient and stable alternatives to lead-based perovskites has proven challenging.[13] For example, the substitution of Pb^{2+} by same-group elements Sn or Ge yields compounds that are unstable, since Sn and Ge prefer the +4 oxidation state.[14] In principle one may try to replace Pb by other +2 cations, but an extensive computational screening showed that no other stable ABX_3 halide perovskite matches the opto-electronic properties of $MAPbI_3$.[15] More recently, the replacement of lead by two heterovalent cations in a double perovskite structure, $A_2BB'X_6$, has been proposed.[16–18] To date four inorganic halide double perovskites ($Cs_2BiAgCl_6$, $Cs_2BiAgBr_6$, $Cs_2InAgCl_6$, $Cs_2SbAgCl_6$)[16–21] and three hybrid halide double perovskites (MA_2BiKCl_6, $MA_2BiTlBr_6$, $MA_2BiAgBr_6$) have been synthesized.[22–24] Recent efforts were also devoted to mix the B-site cations in order to achieve band gap tunability.[25,26] Among the stoichiometric compounds, only $Cs_2InAgCl_6$ and $MA_2BiTlBr_6$ exhibit direct band gaps. However, $Cs_2InAgCl_6$ has a large band gap, 3.3 eV, and $MA_2BiTlBr_6$ contains Tl, which is toxic. Therefore, these lead-free alternatives to $MAPbI_3$ are less attractive for solar cells and optoelectronic devices.

In this work we consider the question on how to make lead-free $A_2B^+B^{3+}X_6$ halide double

perovskites with electronic and optical properties as close as possible to those of $MAPbI_3$. The key requirements that we look for are (i) a direct band gap, (ii) low and balanced effective masses, (iii) high absorption coefficient in the visible, and (iv) a compound that is stable against decomposition. Using a combination of elementary inorganic chemistry considerations and *ab initio* calculations of phase diagrams, electronic and optical properties, we show that the only suitable combination for achieving electronic properties comparable to $MAPbI_3$ is to have In as B^+ cation, and Bi as B^{3+} cation. Furthermore, we show that in order to stabilize the double perovskite structure it is necessary to move beyond elemental A-site cations, and to use either MA or FA or their mixes. Based on these findings we propose that the mixed-cation double perovskites $(Cs/MA/FA)_2InBiBr_6$ will be the most promising route to achieving lead-free perovskites with properties comparable to the best compounds available today, such as direct band gaps in the visible, low effective masses and sharp absorption onset.

In $A_2B^+B^{3+}X_6$ compounds the A-site cation acts mostly as a spacer, and its electronic states are located far from the band edges. This is similar to what happens in ABX_3 perovskites.[27] The halogens at the X site (F, Cl, Br, I) are known to modulate the band gap, so that the gap decreases with increasing ionic radius of the anion.[28] Importantly, neither the A-site nor the X-site elements modify the orbital character and direct/indirect nature of the fundamental gap. Therefore, in order to design materials with direct gap, low effective masses, and strong dipole oscillator strengths, we must focus on the B^+ and B^{3+} cations.

In a previous work we considered $Cs_2BB'X_6$ double perovskites, with B = Bi, Sb, B′ = Cu, Ag, Au, and X = Cl, Br, I.[16] Electronic structure calculations indicated that all these combinations would yield indirect band gaps in the visible range if the compounds were stable. The indirect nature of the gaps is closely related to the formal valency of the B and B′ cations. For example, in $Cs_2BiAgCl_6$ the top of the valence band stems from the filled Ag-4d shell and the filled Bi-6s and 5d shells. The hybridization of Ag-d and Bi-s states via the Cl ligands brings the top of the band to the X point of the fcc Brillouin

zone.[16,19] If we artificially lower the s-states of Bi in a Gedankenexperiment, then we are left with an interaction between Ag-d and Bi-d states, the valence band top moves to the Γ point, and the band gap becomes direct.[20] This observation led us to design and make a new double perovskites, $Cs_2InAgCl_6$, where In^{3+} and Ag^+ have both filled $4d$ shells and empty $5s$ and $5p$ shells in their formal oxidation states.[20] As expected, this new double perovskites exhibits a direct gap at Γ. However, in this case the presence of d-states at the valence band top also introduces a non-dispersive band that hinders charge carrier transport and facilitates the formation of deep defects. In fact, the as-synthesized compound was found to exhibit photochromic behavior, and the optical measurements revealed absorption well-below the band gap, both features that are consistent with the presence of deep defects.[20] Taken together, these observations suggest that in order to engineer a direct gap and well-dispersive bands, we should avoid d states altogether at the band extrema.

Following this general guideline we proceed to examine possible candidates for the B^+ and B^{3+} in $A_2BB'X_6$ double perovskites. For this we consider in turn all the elements that are found in elpasolites.[13,29–31] For the B^{3+} site the possibilities include (i) several transition metals (Sc-Cu, Y and Au), (ii) the lanthanides, (iii) some actinides (Pu, Am and Bk), (iv) the elements of Group III, and (v) the pnictogens. Among these candidates, transition metals, lanthanides, and actinides have partially-occupied d or f orbitals, therefore we would expect to find such states at the band extrema. Similarly, elements belonging to Group III will have the highest occupied states of d character in their +3 oxidation state, therefore we would expect d states at the top of the valence band. Pnictogens stand out in this list, because in their +3 state they have occupied s and d shell and unoccupied p shell, with the d electrons deeper than the s electrons. Therefore in this case we expect s states at the valence band top, and p states at the conduction band bottom. This is analogous to what happens in $MAPbI_3$.[32] Among the pnictogens, N^{3+} and P^{3+} are very small cations, and as a result they would not be stable in a perovskite structure according to Goldschmidt's rules (we estimate Goldschmidt's octahedral factors of 0.12 and 0.34 for NF_6 and PF_6 octahedra,

respectively, well below the stability limit of 0.41).[33] Arsenic is toxic, and as such it is not a good alternative to Pb. Thus, the two larger member of the pnictogen family, Sb^{3+} and Bi^{3+}, remain the only promising candidates to realize double perovskites with electronic structure similar to $MAPbI_3$.

For the B^+ site in $A_2BB'X_6$, the possible candidates are (i) the alkali metals, (ii) the noble metals, and (iii) the elements of Group III. Alkali metals usually lead to non dispersive bands,[22] therefore they are not useful in the present context. Cations of noble metals in the +1 oxidation state have the highest occupied orbitals of *d*-character. This is expected to lead to valence band maxima of *d* character, which is not desirable. On the other hand, the elements of Group III in their +1 oxidation state have filled *s* and *d* shells, with *d* electrons deeper than *s* electrons. This configuration is analogous to the case of Pb in $MAPbI_3$ and is ideal for our purposes. Among Group III elements, the +1 oxidation state tends to be stable only for the largest members of the group. For example In and Tl can be found in the +1 state, while Ga can be found in the +1 state only at high temperature.[34] Since Tl is toxic, we are left with In^+ as the sole candidate for the B^+ site in lead-free halide double perovskites. The conceptual screening just described is summarized in Figure 1.

In the following we investigate the stability, electronic, and optical properties of double perovskites of the type A_2InBiX_6 and A_2InSbX_6 with A = K, Rb or Cs, and X = F, Cl, Br or I. We first examine the empirical Goldschmidt's structure factors, namely the octahedral factor $\mu = r_B/r_X$ and the tolerance factor $t = (r_A + r_B)/\sqrt{2}(r_B + r_X)$, with r_A, r_B, and r_X denoting ionic radii.[35] We consider the octahedral factor for each type of octahedron, and we average the ionic radii of the B and B′ site for the tolerance factor. Of the 36 hypothetical structures considered, all In/X and Bi/X combinations pass the octahedral factor test ($\mu > 0.41$), as well as the combinations Sb/F and Sb/Cl, while Sb/Br and Sb/I are to be discarded. All these combinations pass the tolerance factor test ($0.75 < t < 1.0$).[36] This pre-screening leaves us with 18 potential double perovskites.

As the next step, we perform first-principles calculations to investigate the stability of

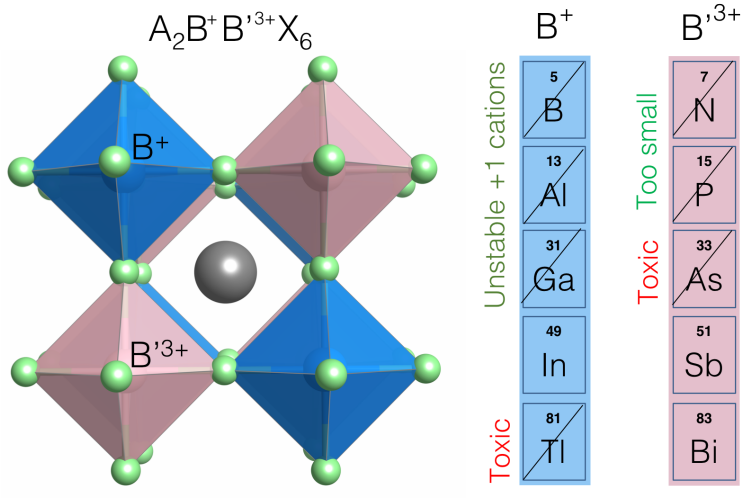

Figure 1: Ball, stick, and polyhedra model of $A_2BB'X_6$ elpasolite (cation-ordered double perovskite) in the cubic structure, within the $Fm\bar{3}m$ space group. The columns on the right illustrate the elements that can be used as B^+ or B^{3+} sites, under the constraint that no d or f electrons appear among the highest occupied or lowest unoccupied orbitals. Among the ten possible options, only In^+, Sb^{3+} and Bi^{3+} are not toxic, can be stable in the required oxidation state, and match Goldschmidt's criteria for structural stability.

these 18 hypothetical compounds against decomposition. To this aim we interrogate the Materials Project database[37] and compare all possible decomposition pathways, as shown in Table 1. Most of the hypothetical double perovskites considered here are found to be unstable within the compound space of the Materials Project database, with the exception of $Rb_2InSbCl_6$, $Rb_2InBiCl_6$, Cs_2InBiF_6 and $Cs_2InBiBr_6$. While this is seemingly good news, we should be careful to consider that our compounds may decompose into reaction products may not included in the Materials Project or even in the Inorganic Crystal Structure Database, ICSD.[38] This is especially important since the redox mechanism of In in these compounds was shown to play a key role.[39]

In order to address this lack of information, we calculate the total energies of hypothetical $A_3B_2X_9$ compounds with A = Rb, Cs, B = In, Sb, Bi, and X = F, Cl, Br. These compounds have been selected in order to complete the Materials Project data in Table 1 with all possible combinations of A, B, and X. In our calculations we make the assumption that these compounds have the same crystal structure as $Cs_3Bi_2Br_9$,[40] and that $A_3In_2X_9$ compounds

Table 1: Decomposition energies (ΔE) and associated decomposition pathways of hypothetical In/Bi and In/Sb halide double perovskite. The decomposition pathways are generated from the Materials Project database. The asterisk denotes a decomposition route where the reaction products are not reported in the Materials Project of the International Crystal Structure Database (ICSD). A negative number indicates that the structure is predicted to decompose.

Compound	ΔE (meV/atom)	Decomposition Pathway
K_2InSbF_6	-163	$4/15\ KIn_2F_7 + 1/3\ KSbF_4 + 7/15\ K_3InF_6 + 2/3\ Sb$
$K_2InSbCl_6$	-95	$7/15\ SbCl_3 + 1/15\ In_5Cl_9 + 2/3\ K_3InCl_6 + 8/15\ Sb$
Rb_2InSbF_6	-73	$1/3\ Rb_2In_3F_{11} + 7/6\ RbF + 1/6\ RbSb_2F_7 + 2/3\ Sb$
$Rb_2InSbCl_6$	-58*	$1/2\ Rb_3In_2Cl_9 + 1/6\ Rb_3Sb_2Cl_9 + 2/3\ Sb$
Cs_2InSbF_6	-17	$2/5\ CsF + 4/5\ CsInF_3 + 4/5\ CsSbF_4 + 1/5\ InSb$
$Cs_2InSbCl_6$	-57	$1/2\ Cs_3In_2Cl_9 + 1/6\ Cs_3Sb_2Cl_9 + 2/3\ Sb$
K_2InBiF_6	-134	$1/3\ KInF_7 + 1/3\ K_2BiF_5 + 1/3\ K_3InF_6 + 2/3\ Bi$
$K_2InBiCl_6$	-61	$3/22\ Bi_6Cl_7 + 2/11\ BiCl_3 + 1/6\ In_2Cl_3 + 2/3\ K_3InCl_6$
$K_2InBiBr_6$	-60	$1/3\ BiBr_3 + KInBr_4 + KBr + 2/3\ Bi$
K_2InBiI_6	-64	$2KI + InI + BiI_3$
Rb_2InBiF_6	-42	$1/3\ RbBiF_4 + RbF + 1/3\ Rb_2In_3F_{11} + 2/3\ Bi$
$Rb_2InBiCl_6$	-43*	$1/2\ Rb_3In_2Cl_9 + 1/6\ Rb_3Bi_2Cl_9 + 2/3\ Bi$
$Rb_2InBiBr_6$	-26	$2/3\ Rb_3BiBr_6 + InBr_2 + 1/3\ Bi$
Rb_2InBiI_6	-36	$1/6\ Rb_3Bi_2I_9 + 1/2\ RbI + RbInI_4 + 2/3\ Bi$
Cs_2InBiF_6	-28*	$1/2\ Cs_3In_2F_9 + 1/6\ Cs_3Bi_2F_9 + 2/3\ Bi$
$Cs_2InBiCl_6$	-24	$1/2\ Cs_3In_2Cl_9 + 1/6\ Cs_3Bi_2Cl_9 + 2/3\ Bi$
$Cs_2InBiBr_6$	-1*	$1/2\ Cs_3In_2Br_9 + 1/6\ Cs_3Bi_2Br_9 + 2/3\ Bi$
Cs_2InBiI_6	-12	$1/2\ CsI + 1/2\ Cs_3Bi_2I_9 + InI$
$Fr_2InBiBr_6$	7	$1/2\ Fr_3In_2Br_9 + 1/6\ Fr_3Bi_2Br_9 + 2/3\ Bi$

have the same structure as $Cs_3In_2Cl_9$.[30] The decomposition pathways involving hypothetical reaction products are indicated by an asterisk in Table 1. After including these additional reactions, we obtain the disappointing result that most halide double perovskites A_2InBiX_6 and A_2InSbX_6 with A = K, Rb or Cs, and X = F, Cl, Br or I will tend to spontaneously decompose into compounds where In in its +3 oxidation state.

Among all the hypothetical double perovskites considered, $Cs_2InBiBr_6$ exhibits the smallest decomposition energy, 1 meV/atom. This result is in agreement with previous calcula-

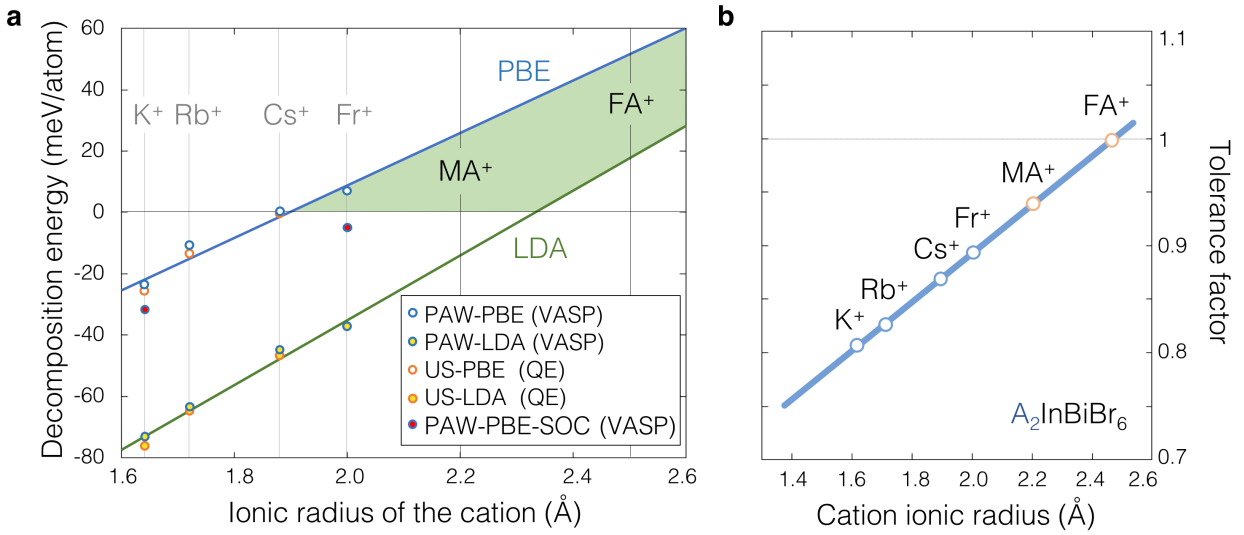

Figure 2: Decomposition energies and tolerance factors for $A_2InBiBr_6$ double perovskites. (a) Decomposition energy vs. the size of the A-site cation, for the reaction $A_2InBiBr_6 \rightarrow 1/2A_3In_2Br_9 + 1/6A_3Bi_2Br_9 + 2/3Bi$. We report the results of calculations using a variety of settings: LDA or PBE exchange and correlation, and ultra-soft pseudopotentials (US) or the projector augmented wave method (PAW). For completeness we also include two calculations performed by including spin-orbit interactions (SOC). The lines are least-square fits to all data-points (without SOC), and the green area indicates the stability region where we expect to find stable In/Bi double perovskites. (b) Goldschmidt's tolerance factor t evaluated for cations of varying size. The dotted horizontal line shows $t = 1$, which corresponds to the ideal cubic perovskite structure. MA stands for methylammonium and FA is formamidinium.

tions.[39,41] The very close proximity of this compound to a stable phase suggests that a slightly-modified version of $Cs_2InBiBr_6$ might be amenable to synthesis. In order to test this hypothesis, we investigate the trends of the decomposition energies as a function of the A-site, B-site, and X-site ions. Surprisingly Figure 2a shows that the energy gain of the reaction $A_2InBiBr_6 \rightarrow {}^1/_2\,A_3In_2Br_9 + {}^1/_6\,A_3Bi_2Br_9 + {}^2/_3\,Bi$ decreases as the size of the A-site cation increases. In order to be more confident about this trend we repeated the calculations using either the local density approximations (LDA) to density functional theory (DFT) or the generalized gradient approximation (PBE), as well as using either ultra-soft (US) pseudopotentials or the projector augmented wave (PAW) method, as described in the Methods. The trend in Figure 2a indicates that it should be possible to stabilize these double perovskites by using A-site cations larger than Cs. In particular, by extrapolating the

curve of decomposition energy vs. the ionic radius of the A cation, we find that the organic cations used in the best photovoltaic perovskites, such as MA and FA ($r_A = 2.2$ Å and 2.5 Å, respectively),[42] should yield structures which are stable against decomposition.

The calculation of phase diagrams of hybrid organic-inorganic perovskites is very challenging due to the sensitivity of the results to the orientation of the organic cations, as well as the lack of detailed structural information on the molecular salt precursors. In order to prove our point we circumvent this difficulty by performing a calculation on the 'hypothetical' double perovskite $Fr_2InBiBr_6$. *We emphasize that Fr is radioactive and obviously not suitable for applications: we choose it merely for a computational experiment, since it is the only +1 elemental cation with an ionic radius larger than Cs.* By performing total energy calculations we find that the replacement of Cs by Fr improves the stability of the double perovskite against decomposition, thereby fully validating the trend anticipated in Figure 2a. This calculation demonstrates that indeed larger cations should make the halide double perovskite $A_2InBiBr_6$ stable against decomposition. For completeness we also show in Figure 2b the empirical tolerance factors. We can see that all the compounds fall within the empirical stability region, with FA lying at the edge of this region. Our findings indicate that mixes of $MA_2InBiBr_6$ and $FA_2InBiBr_6$, and even possibly with a small fraction of $Cs_2InBiBr_6$, should be amenable to synthesis.

We emphasize that, due to the uncertainty in the DFT energetics associated with the choice of the exchange and correlation functional, it is not possible at present to pinpoint the exact mixing fraction of Cs/MA/FA that will lead to stable double perovskites. All we can say is that we have strong evidence for the existence of a 'stability region' (the green area in Figure 2a) where it should be possible to find stable organic-inorganic double perovskites. Based on the data at hand we expect to find stable compounds around compositions like $(MA_{0.5}FA_{0.5})_2InBiBr_6$.

Having identified the most promising compositions to achieve stable double perovskites without *d* states at the band edges, we proceed to analyze their electronic and optical prop-

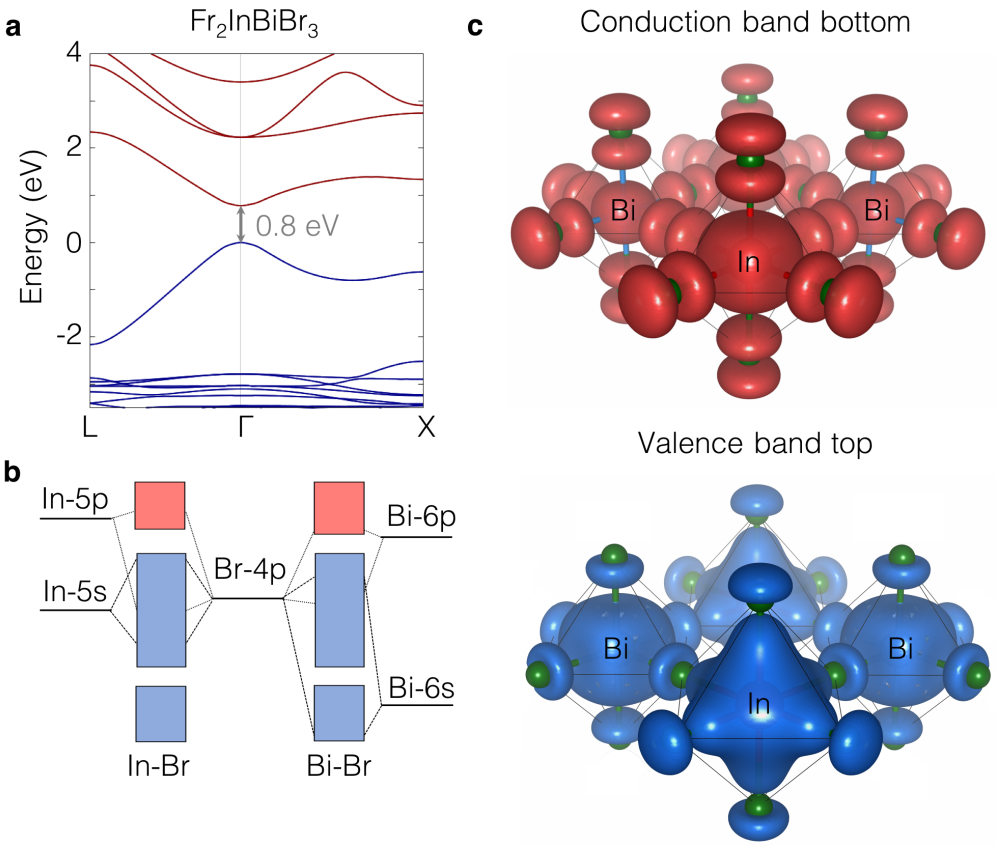

Figure 3: Electronic properties of the 'hypothetical' cubic halide double perovskite $Fr_2InBiBr_6$. (a) Band structure of $Fr_2InBiBr_6$ using the PBE0 hybrid functional. Occupied bands are shown in blue and unoccupied bands are in red. (b) Square modulus of the electronic wavefunctions at the top of the valence band (blue) and at the bottom of the conduction band (red). We see that the wavefunctions extend along all three spatial directions, unlike previously-reported compounds such as $Cs_2InAgCl_6$.[20] (c) Schematic molecular orbital diagram of $Fr_2InBiBr_6$. *We emphasize that we consider Fr because it is the only +1 elemental cation with an ionic radius larger than Cs; Fr is radioactive and is not suitable for applications.*

erties. We start from $Fr_2InBiBr_6$ as the simplest compound that is expected to be stable, even though Fr cannot be used for real applications. We optimize the structure in the elpasolite lattice, with space group $Fm\bar{3}m$.[16] The electronic band structure at the DFT/PBE0 level is shown in Figure 3a. We find highly dispersive bands, with small, isotropic, and balanced effective masses: m_h^*=0.07 m_e, m_e^*=0.08 m_e. These values are comparable with those of $MAPbI_3$.[43] The dispersive character of the bands is a result of the continuous overlap between In-5s, Bi-6p, Br-4p states in the valence, and In-5p, Bi-6p, Br-4p states in the

conduction, see the molecular orbital diagram in Figure 3b. In contrast to In/Ag halide double perovskites,[20] here the wavefunctions exhibit a distinctly three-dimensional character, as shown in Figure 3c.[44]

Having established that the electronic structure of $Fr_2InBiBr_6$ is very similar to $MAPbI_3$, we move on to investigate the hybrid double perovskite $MA_2InBiBr_6$. In this case the orientation of the organic cations is well-known to lead to artifacts such as unphysical distortions of the octahedra, artificial ferroelectric polarization, and artificial breaking of inversion symmetry, leading to Rashba-type spin-orbit splitting of the bands.[45,46] In order to avoid these artifacts, we start from the structural data available for the low-temperature orthorhombic *Pnma* phase of $MAPbI_3$,[47] and replace the four Pb atoms in the unit cell with Bi and In, alternating in a rock-salt sublattice. The optimized structure is shown in Figure 4a. We find that $MA_2InBiBr_6$ retains similar octahedral tilt angles as $MAPbI_3$, and the unit-cell volume is only slightly smaller. The $BiBr_6$ octahedra are found to be slightly smaller than $InBr_6$ octahedra (the BX bond lengths are 2.9 Å vs. 3.3-3.4 Å, respectively). The band structure of $MA_2InBiBr_6$ is shown in Figure 4, alongside with the band structure of $MAPbI_3$ for comparison. The calculated band gap of $MAPbI_3$ is 1.9 eV within DFT/PBE0, in good agreement with higher-level calculations[48] and experiment.[49] The band gap of $MA_2InBiBr_6$ within the same level of approximation is only slightly larger, 2.0 eV. We recall that band gaps tend to be larger in the presence of octahedral tilts,[27,50] hence the high-temperature cubic structures are expected to exhibit smaller gaps.

Figure 4b shows the calculated optical absorption spectrum of $MA_2InBiBr_6$, as well as calculations for prototypical photovoltaic materials such as Si, GaAs, and $MAPbI_3$. It is evident that $MA_2InBiBr_6$ is a strong optical absorber, and behaves essentially like $MAPbI_3$. The striking similarity between the electronic and optical properties of $MAPbI_3$ and $MA_2InBiBr_6$ shown in Figure 4 provides a strong validation of the design rules discussed in this work.

In order to probe the effects of mixing cations at the A site, we construct models of $(Cs_{0.5}MA_{0.5})_2InBiBr_6$ and $(MA_{0.5}FA_{0.5})_2InBiBr_6$ by replacing two out of four MA cations in

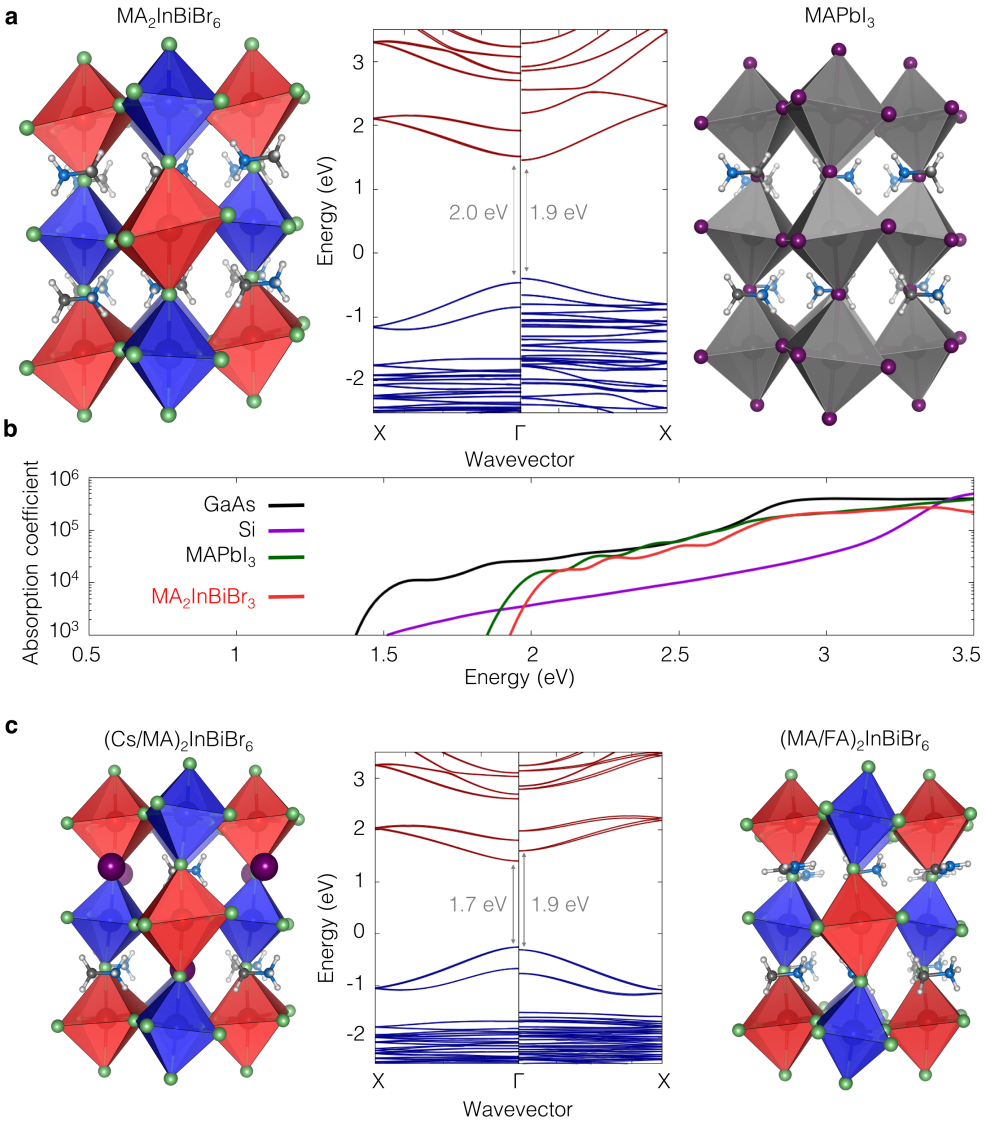

Figure 4: Electronic and optical properties of 'hypothetical' halide double perovskites $MA_2InBiBr_6$, $(Cs/MA)_2InBiBr_6$, and $(MA/FA)_2InBiBr_6$. (a) Ball-stick-octahedra models of the optimized structures and band structures of $MA_2InBiBr_6$ (left) and $MAPbI_3$ (right). (b) Calculated optical absorption coefficients of $MA_2InBiBr_6$ (red), Si (purple), GaAs (black), and $MAPbI_3$ (green). (c) Same as in (a), but for $(Cs/MA)_2InBiBr_6$ and $(MA/FA)_2InBiBr_6$. MA stands for methylammonium and FA is formamidinium.

$MA_2InBiBr_6$ with Cs or FA, respectively. We choose to alternate the two types of cations in a rock-salt A-site sublattice, so as to maintain inversion symmetry. The optimized model structures are shown in Figure 4c. The band structure of these compounds (Figure 4c) remains very similar to that of $MAPbI_3$, with band gaps of 1.7 eV $[(Cs_{0.5}MA_{0.5})_2InBiBr_6]$ and

1.9 eV [$(FA_{0.5}MA_{0.5})_2InBiBr_6$]. This suggests that, on top of being stable against decomposition, mixed-cation double perovskites should also offer band gap tunability across the visible range, precisely as in the case of (Cs/MA/FA)PbI_3.[51,52]

In conclusion, we identified a promising pathway to synthesize stable lead-free halide double perovskites with optoelectronic properties comparable to those of $MAPbI_3$. By combining notions of elementary inorganic chemistry with *ab initio* calculations of phase stability, electronic structure, and optical properties, we identified the mixed cation double perovskite $(Cs/MA/FA)_2InBiBr_6$ as a potential replacement for $MAPbI_3$. Our key novel observation is that the most problematic instability, namely the oxidation of In^+ into In^{3+}, becomes energetically less favorable as the size of the A-site cation increases. This finding rules out all-inorganic double perovskites as potential replacements for $MAPbI_3$, and indicates that the road for Pb-free perovskites solar cells goes through organic-inorganic hybrid systems. The present work urgently calls for a detailed experimental campaign to attempt the synthesis and characterization of $(Cs/MA/FA)_2InBiBr_6$ across an extensive range of Cs/MA/FA compositions.

Computational Methods: DFT calculations were performed using Quantum ESPRESSO[53] and VASP.[54] For structural properties we employed the PBE[55] or the LDA[56] exchange and correlation, and for band structures we used the PBE0 functional.[57] We employed the PAW method[58] in VASP, and US pseudopotentials in Quantum ESPRESSO.[59] We include In $4d$ semicore states in all calculations, and all band structures are fully relativistic.[16,60] The following planewaves kinetic energy cutoffs were employed: 38 Ry for PAW/LDA, 38 Ry for PAW/PBE, 40 Ry for US/LDA, 40 Ry for US/PBE and 22 Ry for the PAW/PBE0. The Brillouin zone was sampled as follows: 15^3 Γ-centered grid for the structural relaxations; 6^3 grid for the PBE0 calculations; 15^3 grid for optical absorption. The band structures were calculated using DFT/PBE, and scissor-corrected using the PBE0 gaps. The effective masses were calculated using fully-relativistic DFT/PBE0 using finite differences. The calculation of the absorption coefficient was performed within the independent-particle approximation, using

YAMBO,[61] the LDA, and fully-relativistic norm-conserving pseudopotentials;[62] the spectra were scissor-corrected using the PBE0 gaps. The decomposition pathways were identified using Pymatgen[63] and the Materials Project,[37] and all energies except those marked by asterisks in Table 1 are from the Materials Project.

Acknowledgement

The authors are indebted with Marios Zacharias for sharing the calculated absorption coefficients of Si and GaAs included in Figure 4b. The research leading to these results has received funding from the Graphene Flagship (Horizon 2020 grant no. 696656 - GrapheneCore1), the Leverhulme Trust (Grant RL-2012-001), the UK Engineering and Physical Sciences Research Council (Grant No. EP/M020517/1, EP/M014797/1, EP/M024881/1). The authors acknowledge the use of the University of Oxford Advanced Research Computing (ARC) facility (http://dx.doi.org/10.5281/zenodo.22558) and the ARCHER UK National Supercomputing Service under the 'AMSEC' Leadership project and the DECI resource 'Cartesius' based in the Netherlands at SURFsara with support from the PRACE AISBL.

References

(1) Green, M. A.; Ho-Baillie, A.; Snaith, H. J. The Emergence of Perovskite Solar Cells. *Nat. Photon.* **2014**, *8*, 506–514.

(2) Suntivich, J.; Gasteiger, H. A.; Yabuuchi, N.; Nakanishi, H.; Goodenough, J. B.; Shao-Horn, Y. Design Principles for Oxygen-Reduction Activity on Perovskite Oxide Catalysts for Fuel Cells and Metal-Air Batteries. *Nat. Chem.* **2011**, *3*, 546–550.

(3) Wang, N.; Cheng, L.; Ge, R.; Zhang, S.; Miao, Y.; Zou, W.; Yi, C.; Sun, Y.; Cao, Y.; Yang, R. et al. Perovskite Light-Emitting Diodes Based on Solution-Processed Self-Organized Multiple Quantum Wells. *Nat. Photon.* **2016**, *10*, 699–704.

(4) Park, S.; Chang, W. J.; Lee, C. W.; Park, S.; Ahn, H.-Y.; Nam, K. T. Photocatalytic Hydrogen Generation from Hydriodic Acid using Methylammonium Lead Iodide in Dynamic Equilibrium with Aqueous Solution. *Nat. Energy* **2016**, *2*, 16185.

(5) Bellaiche, L.; Vanderbilt, D. Virtual Crystal Approximation Revisited: Application to Dielectric and Piezoelectric Properties of Perovskites. *Phys. Rev. B* **2000**, *61*, 7877–7882.

(6) Fine, G. F.; Cavanagh, L. M.; Afonja, A.; Binions, R. Metal Oxide Semi-Conductor Gas Sensors in Environmental Monitoring. *Sensors* **2010**, *10*, 5469–5502.

(7) Bednorz, J. G.; Müller, K. A. Possible HighTc Superconductivity in the BaLaCuO System. *Z. Phys. B Con. Mat.* **1986**, *64*, 189–193.

(8) Kojima, A.; Teshima, K.; Shirai, Y.; T., M. Organometal Halide Perovskites as Visible-Light Sensitizers for Photovoltaic Cells. *J. Am. Chem. Soc.* **2009**, *131*, 6050.

(9) Lee, M. M.; Teuscher, J.; Miyasaka, T.; Myrakami, T. N.; Snaith, H. J. Efficient Hybrid Solar Cells Based on Meso-Superstructured Organometal Halide Perovskites. *Science* **2012**, *338*, 643.

(10) Kim, H.-S.; Lee, C. R.; Im, J.-H.; Lee, K.-B.; Moehl, T.; Marchioro, A.; Moon, S.-J.; Humphry-Baker, R.; Yum, J.-H.; Moser, J. E. et al. Lead Iodide Perovskite Sensitized All-Solid-State Submicron Thin Film Mesoscopic Solar Cell with Efficiency Exceeding 9%. *Sci. Rep.* **2012**, *2*, 591.

(11) Seo, J.; Noh, J. H.; Seok, S. I. Rational Strategies for Efficient Perovskite Solar Cells. *Accounts Chem. Res.* **2016**, *49*, 562–572.

(12) Berhe, T. A.; Su, W.-N.; Chen, C.-H.; Pan, C.-J.; Cheng, J.-H.; Chen, H.-M.; Tsai, M.-C.; Chen, L.-Y.; Dubale, A. A.; Hwang, B.-J. Organometal Halide Perovskite Solar Sells: Degradation and Stability. *Energy Environ. Sci.* **2016**, *9*, 323–356.

(13) Giustino, F.; Snaith, H. J. Toward Lead-Free Perovskite Solar Cells. *ACS Energy Lett.* **2016**, *1*, 1233–1240.

(14) Noel, N.; Stranks, S. D.; Abate, A.; Wehrenfennig, C.; Guarnera, S.; Haghighirad, A.-A.; Sadhanala, A.; Eperon, G. E.; Pathak, S. K.; Johnston, M. B. et al. Lead-Free Organic-Inorganic Tin Halide Perovskite for Photovoltaic Applications. *Energ. Environ. Sci* **2014**, *7*, 3061.

(15) Filip, M. R.; Giustino, F. Computational Screening of Homovalent Lead Substitution in OrganicInorganic Halide Perovskites. *J. Phys. Chem. C* **2016**, *120*, 166–173.

(16) Volonakis, G.; Filip, M. R.; Haghighirad, A. A.; Sakai, N.; Wenger, B.; Snaith, H. J.; Giustino, F. Lead-Free Halide Double Perovskites via Heterovalent Substitution of Noble Metals. *J. Phys. Chem. Lett.* **2016**, *7*, 1254–1259.

(17) Slavney, A. H.; Hu, T.; Lindenberg, A. M.; Karunadasa, H. I. A Bismuth-Halide Double Perovskite with Long Carrier Recombination Lifetime for Photovoltaic Applications. *J. Am. Chem. Soc.* **2016**, *138*, 2138–2141.

(18) McClure, E. T.; Ball, M. R.; Windl, W.; Woodward, P. M. Cs_2AgBiX_6 (X = Br, Cl) New Visible Light Absorbing, Lead-Free Halide Perovskite Semiconductors. *Chem. Mater.* **2016**, *28*, 1348–1354.

(19) Filip, M. R.; Hillman, S.; Haghighirad, A. A.; Snaith, H. J.; Giustino, F. Band Gaps of the Lead-Free Halide Double Perovskites $Cs_2BiAgCl_6$ and $Cs_2BiAgBr_6$ from Theory and Experiment. *J. Phys. Chem. Lett.* **2016**, *7*, 2579–2585.

(20) Volonakis, G.; Haghighirad, A. A.; Milot, R. L.; Sio, W. H.; Filip, M. R.; Wenger, B.; Johnston, M. B.; Herz, L. M.; Snaith, H. J.; Giustino, F. Cs2InAgCl6: A New Lead-Free Halide Double Perovskite with Direct Band Gap. *J Phys. Chem. Lett.* **2017**, *8*, 772–778.

(21) Tran, T. T.; Panella, J. R.; Chamorro, J. R.; Morey, J. R.; McQueen, T. M. Designing Indirect-Direct Bandgap Transitions in Double Perovskites. *Mater. Horiz.* **2017**, –.

(22) Wei, F.; Deng, Z.; Sun, S.; Xie, F.; Kieslich, G.; Evans, D. M.; Carpenter, M. A.; Bristowe, P. D.; Cheetham, A. K. The Synthesis, Structure and Electronic Properties of a Lead-Free Hybrid Inorganic-Organic Double Perovskite (MA)2KBiCl6 (MA = Methylammonium). *Mater. Horiz.* **2016**, *3*, 328–332.

(23) Deng, Z.; Wei, F.; Sun, S.; Kieslich, G.; Cheetham, A. K.; Bristowe, P. D. Exploring the Properties of Lead-Free Hybrid Double Perovskites using a Combined Computational-Experimental Approach. *J. Mater. Chem. A* **2016**, *4*, 12025–12029.

(24) Wei, F.; Deng, Z.; Sun, S.; Zhang, F.; Evans, D. M.; Kieslich, G.; Tominaka, S.; Carpenter, M. A.; Zhang, J.; Bristowe, P. D. et al. Synthesis and Properties of a Lead-Free Hybrid Double Perovskite: (CH3NH3)2AgBiBr6. *Chem. Mater.* **2017**, *29*, 1089–1094.

(25) Slavney, A. H.; Leppert, L.; Bartesaghi, D.; Gold-Parker, A.; Toney, M. F.; Savenije, T. J.; Neaton, J. B.; Karunadasa, H. I. Defect-Induced Band-Edge Reconstruction of a Bismuth-Halide Double Perovskite for Visible-Light Absorption. *J. Am. Chem. Soc.* **2017**, *139*, 5015–5018.

(26) Du, K.; Meng, W.; Wang, X.; Yan, Y.; Mitzi, D. B. Bandgap Engineering of Lead-Free Double Perovskite Cs2AgBiBr6 through Trivalent Metal Alloying. *Angew. Chem. Int. Edit.* **2017**, DOI:10.1002/anie.201703970.

(27) Filip, M. R.; Eperon, G.; Snaith, H. J.; Giustino, F. Steric Engineering of Metal-Halide Perovskites with Tunable Optical Band Gaps. *Nat. Commun.* **2014**, *5*, 5757.

(28) Noh, J. H.; Im, S. H.; Heo, J. H.; Mandal, T. N.; Seok, S. I. Chemical Management for Colorful, Efficient, and Stable InorganicOrganic Hybrid Nanostructured Solar Cells. *Nano Lett.* **2013**, *13*, 1764–1769.

(29) Meyer, G. Halo-Elpasolites. VI. The First-Iodo-Elpasolites, $CsB^{I}M^{III}I_6$ (B^{I}=Li, Na). *Z. Naturforsch. B* **1980**, *35*, 268–276.

(30) Meyer, G. Zur Kenntnis der Chloro- und Bromo-Indate (III). A3In2Cl9 (A = Cs, Rb, In, Tl) und Cs3In2Br9x Clx (x = 0, 3, 6, 7, 8). *Z. Anor. Allg Chem.* **1978**, *445*, 140–146.

(31) Morss, L. R.; Siegal, M.; Stenger, L.; Edelstein, N. Preparation of Cubic Chloro Complex Compounds of Trivalent Metals: Cs_2NAMCl_6. *Inorg. Chem.* **1970**, *9*, 1771–1775.

(32) Umebayashi, T.; Asai, K.; Kondo, T.; Nakao, A. Electronic Structures of Lead Iodide Based Low-Dimensional Crystals. *Phys. Rev. B* **2003**, *67*, 155405.

(33) Rohrer, G. *Structure and Bonding in Crystalline Materials*; Cambridge University Press: Cambridge, 2001.

(34) Dohmeier, C.; Loos, D.; Schnockel, H. Aluminum(I) and Gallium(I) Compounds: Syntheses, Structures, and Reactions. *Angew. Chem. Int. Edit.* **1996**, *35*, 129–149.

(35) Goldschmidt, V. M. Die Gesetze der Krystallochemie. *Naturwissenschaften* **1926**, *14*, 477–485.

(36) Li, C.; Lu, X.; Ding, W.; Feng, L.; Gao, Y.; Guo, Z. Formability of ABX_3 (X = F, Cl, Br, I) Halide Perovskites. *Acta Cryst. B* **2008**, *64*, 702–707.

(37) Jain, A.; Ong, S. P.; Hautier, G.; Chen, W.; Richards, W. D.; Dacek, S.; Cholia, S.; Gunter, D.; Skinner, D.; Ceder, G. et al. The Materials Project: A Materials Genome Approach to Accelerating Materials Innovation. *APL Mater.* **2013**, *1*, 011002.

(38) Inorganic Crystal Structure Database, FIZ Karlsruhe: Germany. `http://www2.fiz-karlsruhe.de`.

(39) Xiao, Z.; Du, K.-Z.; Meng, W.; Wang, J.; Mitzi, D. B.; Yan, Y. Intrinsic Instability of Cs2In(I)M(III)X6 (M = Bi, Sb; X = Halogen) Double Perovskites: A Combined

Density Functional Theory and Experimental Study. *J. Am. Chem. Soc.* **2017**, *139*, 6054–6057.

(40) Aleksandrova, I.; Burriel, R.; Bartolome, J.; Bagautdinov, B.; Blasco, J.; Sukhovsky, A.; Torres, J.; Vasiljev, A.; Solovjev, L. Low-Temperature Phase Transitions in the Trigonal Modification of Cs 3 Bi 2 Br 9 and Cs 3 Sb 2 I 9. *Phase Transit.* **2002**, *75*, 607–620.

(41) Savory, C. N.; Walsh, A.; Scanlon, D. O. Can Pb-Free Halide Double Perovskites Support High-Efficiency Solar Cells? *ACS Energy Lett.* **2016**, *1*, 949–955.

(42) Kieslich, G.; Sun, S.; Cheetham, A. K. An Extended Tolerance Factor Approach for Organic-Inorganic Perovskites. *Chem. Sci.* **2015**, *6*, 3430–3433.

(43) Filip, M. R.; Verdi, C.; Giustino, F. GW Band Structures and Carrier Effective Masses of CH3NH3PbI3 and Hypothetical Perovskites of the Type APbI3: A = NH4, PH4, AsH4 and SbH4. *J. Phys. Chem. C* **2015**, *119*, 25209–25219.

(44) Xiao, Z.; Meng, W.; Wang, J.; Mitzi, D. B.; Yan, Y. Searching for Promising New Perovskite-Based Photovoltaic Absorbers: the Importance of Electronic Dimensionality. *Mater. Horiz.* **2017**, *4*, 206–216.

(45) Frost, J. M.; Butler, K. T.; Brivio, F.; Hendon, C. H.; van Schilfgaarde, M.; Walsh, A. Atomistic Origins of High-Performance in Hybrid Halide Perovskite Solar Cells. *Nano Lett.* **2014**, *5*, 2584.

(46) Brivio, F.; Butler, K. T.; Walsh, A.; van Schilfgaarde, M. Relativistic Quasiparticle Self-Consistent Electronic Structure of Hybrid Halide Perovskite Photovoltaic Absorbers. *Phys. Rev. B* **2014**, *89*, 155204.

(47) Baikie, T.; Fang, Y.; Kadro, J. M.; Schreyer, M.; Wei, F.; Mhaisalkar, S. G.; Grätzel, M.; White, T. J. Synthesis and Crystal Chemistry of the Hybrid Perovskite ($CH_3NH_3PbI_3$) for Solid-State Sensitized Solar Applications. *J. Chem. Mater. A* **2013**, *1*, 5628.

(48) Filip, M. R.; Giustino, F. GW Quasiparticle Band Gap of the Hybrid Organic-Inorganic Perovskite CH3NH3PbI3: Effect of Spin-Orbit Interaction, Semicore Electrons, and Self-Consistency. *Phys. Rev. B* **2014**, *90*, 245145.

(49) D'Innocenzo, V.; Grancini, G.; Alcocer, M. J. P.; Kandada, A. R. S.; Stranks, S. D.; Lee, M. M.; Lanzani, G.; Snaith, H. J.; Petrozza, A. Excitons Versus Free Charges in Organo-Lead Tri-Halide Perovskites. *Nat. Commun.* **2014**, *5*, 3586.

(50) Herz, L. M. Charge-Carrier Dynamics in Organic-Inorganic Metal Halide Perovskites. *Annu. Rev. Phys. Chem.* **2016**, *67*, 65–89.

(51) McMeekin, D. P.; Sadoughi, G.; Rehman, W.; Eperon, G. E.; Saliba, M.; Hrantner, M. T.; Haghighirad, A. A.; Sakai, N.; Korte, L.; Rech, B. et al. A Mixed-Cation Lead Mixed-Halide Perovskite Absorber for Tandem Solar Cells. *Science* **2016**, *8*, 151–155.

(52) Eperon, G. E.; Leijtens, T.; Bush, K. A.; Prasanna, R.; Green, T.; Jacob Tse-Wei Wang, J. T.-W.; McMeekin, D. P.; Volonakis, G.; Milot, R. L.; May, R. et al. Perovskite-Perovskite Tandem Photovoltaics With Optimized Bandgaps. *Science* **2016**, *354*, 861–865.

(53) Giannozzi, P.; Baroni, S.; Bonini, N.; Calandra, M.; Car, R.; Cavazzoni, C.; Ceresoli, D.; Chiarotti, G.; Cococcioni, M.; Dabo, I. et al. QUANTUM ESPRESSO: A Modular and Open-Source Software Project for Quantum Simulations of Materials. *J. Phys.: Condens. Matter.* **2009**, *21*, 395502.

(54) Kresse, G.; Furthmuller, J. Efficient Iterative Schemes For *ab initio* Total-Energy Calculations Using a Plane-Wave Basis Set. *Phys. Rev. B* **1996**, *54*, 11169–11186.

(55) Perdew, J. P.; Burke, K.; Ernzerhof, M. Generalized Gradient Approximation Made Simple. *Phys. Rev. Lett.* **1996**, *77*, 3865.

(56) Perdew, J. P.; Zunger, A. Self-Interaction Correction to Density-Functional Approximations for Many-Electrons Systems. *Phys. Rev. B* **1981**, *23*, 5048.

(57) Paier, J.; Hirschl, R.; Marsman, M.; Kresse, G. The Perdew-Burke-Ernzerhof Exchange-Correlation Functional Applied to the G2-1 Test Set Using a Plane-Wave Basis Set. *J. Chem. Phys.* **2005**, *122*, 234102.

(58) Blöchl, P. E. Projector Augmented-Wave Method. *Phys. Rev. B* **1994**, *50*, 17953–17979.

(59) Garrity, K. F.; Bennett, J. W.; Rabe, K. M.; Vanderbilt, D. Pseudopotentials for High-Throughput DFT Calculations. *Comput. Mater. Sci.* **2014**, *81*, 446 – 452.

(60) Even, J.; Pedesseau, L.; Jancu, J.-M.; Katan, C. Importance of Spin-Orbit Coupling in Hybrid Organic/Inorganic Perovskites for Photovoltaic Applications. *J. Phys. Chem. Lett.* **2013**, *4*, 2999.

(61) Marini, A.; Hogan, C.; Grüning, M.; Varsano, D. Yambo: An Ab Initio Tool for Excited State Calculations. *Comp. Phys. Commun.* **2009**, *180*, 1392.

(62) Troullier, N.; Martins, J. L. Efficient Pseudopotentials for Plane-Wave Calculations. *Phys. Rev. B* **1991**, *43*, 1993.

(63) Ong, S. P.; Richards, W. D.; Jain, A.; Hautier, G.; Kocher, M.; Cholia, S.; Gunter, D.; Chevrier, V. L.; Persson, K. A.; Ceder, G. Python Materials Genomics (pymatgen): A robust, open-source python library for materials analysis. *Comput. Mater. Sci.* **2013**, *68*, 314 – 319.

Table of Contents Image